Photophysics and Photoinduced Electron-Transfer Reactivity of Ruthenium(II) Complexes with Oligo(thiophene-bipyridine) Ligands[†,1]

Yao Liu,[‡] Antoinette De Nicola,[§] Olivier Reiff,[§] Raymond Ziessel,*[,§] and Kirk S. Schanze*[,‡]

Department of Chemistry, University of Florida, P. O. Box 117200, Gainesville, Florida 32611-7200, and Laboratoire de Chimie Moléculaire, Ecole de Chimie, Polymères, Matériaux (ECPM), Université Louis Pasteur (ULP), 25 Rue Becquerel, 67087 Strasbourg Cedex 02, France

Received: September 11, 2002; In Final Form: January 7, 2003

A novel series of mono-, di-, and trimeric ruthenium(II) complexes has been synthesized in which the quasi-linear polytopic ligand is constituted by 2,2′-bipyridine (bpy) subunits linked in the 5,5′ positions by 2,5-diethynyl-3,4-dibutylthiophene spacers. Each Ru center is capped by two unsubstituted bpy ligands, and the final complexes are soluble and photostable. Cyclic voltammetry was used to assign the first oxidation and the sequential reduction potentials. Oxidation is metal based while the first reduction is based on the thiophene-substituted ligand. The number of ethynyl-thiophene "modules" and the way these modules are substituted strongly influence the photophysical properties of the complexes. In the case of the mononuclear derivatives (**RuT** and **TRuT**), luminescence arises from the MLCT manifold and the thiophene-substituted bpy ligands act as the "acceptor" ligands. The photophysical properties of the di- and trimetallic complexes (**RuTRu** and **RuTRuTRu**) are consistent with an "intraligand" $^3\pi,\pi^*$ excited state, where the excitation is localized on the thiophene−bipyridine oligomeric ligands. The dimeric complex (**RuTRu**) has an especially long lifetime (7.3 μs), presumably because the $^3\pi,\pi^*$ state is more than 0.1 eV below the lowest MLCT configuration. The excited states of all complexes are efficiently quenched by MV^{2+}, with a rate constant ranging from 4×10^7 to 4×10^8 M^{-1} s^{-1}. Analysis of the rate-free energy correlations for the photoinduced electron-transfer reactions indicate that the nature of the lowest excited state (i.e. $^3\pi,\pi^*$ or MLCT) has little or no influence on the dynamics of electron transfer.

Introduction

Conjugated materials are having a significant impact in emerging technologies for electronics, optoelectronics, and biotechnology.[2−8] While most applications of conjugated materials that are presently under development are based on organic materials,[2−8] a number of significant research efforts are focused on the properties of π-conjugated materials that contain transition metals.[9−18] Some of the significant applications that are being considered for metal-containing materials include organic light emitting diodes (OLEDs),[12,13,19−21] laser damage protection,[22,23] and optical signaling.[10,24]

Oligo- and poly(thiophenes) have been at the forefront of electro- and photoactive conjugated materials research.[6,25−28] As part of this effort, considerable work has focused on understanding the photophysical properties of thiophene containing π-conjugated electronic systems.[29−32] Oligo- and poly(thiophenes) typically feature strong fluorescence from a $^1\pi,\pi^*$ singlet excited state. In addition, direct optical excitation of these systems affords a $^3\pi,\pi^*$ state in moderate yields. The triplet states of oligo- and poly(thiophenes) have been characterized by laser flash photolysis,[29−31] and in a few cases phosphorescence has even been observed from polymer samples.[33,34] For alkyl substituted poly(thiophenes) the $^1\pi,\pi^*$ and $^3\pi,\pi^*$ states lie at ca. 2.65 and 1.95 eV, respectively (i.e., the singlet−triplet splitting is $\approx$0.7 eV).[34]

Our groups have an ongoing interest in the synthesis and investigation of the excited-state properties of organic π-conjugated electronic systems that contain transition metals that interact strongly with the π-electron system.[14−16,35−40] As part of this effort, we recently reported a study of a series of conjugated polymers that feature ruthenium(II) and osmium(II) polypyridine complexes interspersed in a poly(3-octylthiophene) backbone.[41] These polymers feature energetically low-lying excited states based on dπ (M) $\rightarrow$ π^* metal-to-ligand charge transfer (MLCT) at the metal complex chromophores, as well as $^3\pi,\pi^*$ state(s) localized on the poly(3-octylthiophene) chain. Photoluminescence and transient absorption studies revealed that, for the Ru(II) polymers, the long-lived excited states were primarily of $^3\pi,\pi^*$ character, but for the Os(II) system the MLCT state dominated the photophysics of the materials.

In the present paper we report a study of a series of structurally well-defined metal complexes featuring ruthenium(II) polypyridine chromophores coordinated to a series of π-conjugated "oligomer ligands" that contain alternating 3,4-dibutylthiophene and 2,2-bipyridine units connected by ethynyl linkages (Chart 1). The study explores the correlation between the conjugation length of the oligomer ligands and the nature of the lowest excited state. All of the complexes display long-lived (i.e., microsecond time scale) and luminescent excited states. On the basis of photoluminescence and transient absorption spectroscopy, it is determined that in two systems the lowest excited state is based on dπ (Ru) $\rightarrow$ π^* (L) MLCT (where L = the dibutylthiophene−bipyridine ligand), while in the other two systems the lowest excited state is $^3\pi,\pi^*$ based on the oligomer

[†] Part of the special issue "George S. Hammond & Michael Kasha Festschrift."

* To whom correspondence should be addressed. E-mails: ziessel@chimie.u-strasbg.fr; kschanze@chem.ufl.edu.

[‡] University of Florida.

[§] Université Louis Pasteur.

10.1021/jp026971d CCC: $25.00
Published on Web 03/28/2003

CHART 1

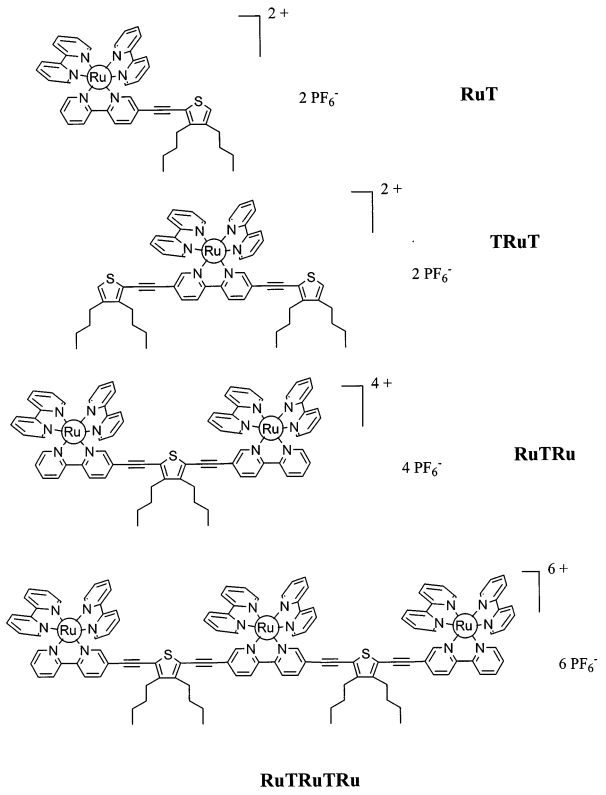

ligand. The results of this study provide insight into how interplay between these two excited states influences the photophysics of the complexes. In addition, this study may provide information that is helpful in the design of new metal−organic materials for optoelectronic applications.

Experimental Section

General Methods. The 200.1 MHz ^{1}H NMR spectra were recorded at room temperature using perdeuterated acetone as solvent and internal standard. Chemical shifts (δ, ppm) are reported relative to residual protiated solvent at 2.05 ppm. FT-IR spectra were recorded as KBr pellets on a Nicolet 210 spectrometer. Chromatographic purification was conducted using 40−63 μm silica gel or aluminum oxide 90 standardized. Thin-layer chromatography (TLC) was performed on silica gel or aluminum oxide plates coated with fluorescent indicator. Deactivated plates were previously treated with 90:10 CH_2Cl_2−Et_3N. All mixtures of solvents are given in v/v ratio.

Materials. CH_2Cl_2 was distilled from CaH_2. EtOH was dried over alumina prior to distillation. KPF_6 was recrystallized from hot EtOH. All ligands bearing substituted 2-ethynyl-3,4-dibutylthiophene (**bpyT** and **TbpyT**) or 2,5-diethynyl-3,4-dibutylthiophene (**bpyTbpy** and **bpyTbpyTbpy**) were prepared according to Sonogashira cross-coupling reactions between adequate building blocks and promoted by low valent palladium-(0). Analytical and spectroscopic data for the free ligands are in agreement with the expected formulas, and full details for the synthetic procedure and characterization is published elsewhere.[40]

General Procedure for the Preparation of the Ruthenium-(II) Complexes. In a Schlenk flask a suspension of the adequate number of *cis*-$[Ru(bpy)_2Cl_2]\cdot 2H_2O$ equivalents in ethanol was gradually added to a stirred dichloromethane solution of the free ligands. The mixture was heated at 60 °C for 12 h. During heating the initially red-violet solution turned red-orange. After complete consumption of the starting material (determined by TLC), an aqueous solution of KPF_6 (5 equiv/(ruthenium center)) was added and the solvent was then removed under vacuum. The precipitate was recovered by centrifugation with water and purified by chromatography on silica eluting with a mixture of acetonitrile/water (85/15 (v/v)) using a gradient of KNO_3 saturated in water from 0.1 to 1%. The fractions containing the pure complex were evaporated to dryness, and the residue was dissolved in a minimum of 90/10 acetone/water (ca. 10 mL). The excess nitrates were eliminated by filtration, and an aqueous solution saturated with KPF_6 was added. Evaporation of the organic solvent afforded a deep-red solid which was recovered by centrifugation, washed successively with water (3 × 10 mL) and diethyl ether, and dried several hours under high vacuum. The analytically pure samples were recrystalized by slow evaporation of acetone from a mixture of acetone and hexane and identified by classical spectroscopic methods as well as by elemental analysis.

RuT. Prepared according to the general conditions, from 0.050 g (0.133 mmol) of **bpyT** and 0.072 g (0.14 mmol) of $[Ru(bpy)_2Cl_2]\cdot 2H_2O$ in 2 mL of CH_2Cl_2 and 10 mL of C_2H_5-OH, to give 0.090 g of **RuT** (56%). ^{1}H NMR: δ 8.83−8.81 (m, 6H), 8.32−8.17 (m, 6H), 8.15−8.02 (m, 6H), 7.65−7.56 (m, 5H), 7.27 (s, thiophene, 1H), 2.68−2.52 (m, 4H), 1.70−1.27 (m, 8H), 0.96−0.85 (m, 6H). FT-IR (KBr, cm^{-1}): 2953 (m), 2927 (m), 2861 (m), 2194 (s, C≡C), 1604 (m), 1594 (m), 1447 (m), 1464 (m), 1429 (m), 1316 (w), 1162 (m), 829 (vs). UV−vis (CH_3CN; λ, nm (ϵ, M^{-1} cm^{-1})): 287 (73 500), 372 (29 500), 453 (12 000). ESI-MS (CH_3CN): 933.3 ($[M - PF_6]^+$, 100%), 394.2 ($[M - 2PF_6]^{2+}$). Anal. Calcd for $C_{44}H_{42}N_6RuSP_2F_{12}$: C, 47.61; H, 3.81; N, 7.57. Found: C, 47.38; H, 3.62; N, 7.38.

TRuT. Prepared according to the general conditions, from 0.045 g (0.078 mmol) of **TbpyT** and 0.045 g (0.083 mmol) of $[Ru(bpy)_2Cl_2]\cdot 2H_2O$ in 3 mL of CH_2Cl_2 and 15 mL of C_2H_5-OH, to give 0.073 g of **TRuT** (73%). ^{1}H NMR: δ 8.89−8.85 (m, 6H), 8.31−8.23 (m, 8H), 8.09−8.08 (m, 4H), 7.67−7.60 (m, 4H), 7.28 (s, thiophene, 2H), 2.68−2.52 (m, 8H), 1.64−1.24 (m, 16H), 0.97−0.85 (m, 12H). FT-IR (KBr, cm^{-1}): 2929 (m), 2860 (m), 2197 (s, C≡C), 1596 (m), 1466 (m), 1446 (m), 1243 (m), 1094 (m), 840 (vs), 802 (m), 764 (m). UV−vis (CH_3-CN; λ, nm (ϵ, M^{-1} cm^{-1})): 287 (61 700), 424 (51 500). ESI-MS (CH_3CN): 1151.3 ($[M - PF_6]^+$, 100%), 503.2 ($[M - 2PF_6]^{2+}$). Anal. Calcd for $C_{58}H_{60}N_6RuS_2P_2F_{12}$: C, 53.74; H, 4.67; N, 6.48. Found: C, 53.38; H, 4.45; N, 6.38.

RuTRu. Prepared according to the general conditions, from 0.055 g (0.100 mmol) of **bpyTbpy** and 0.113 g (0.219 mmol) of $[Ru(bpy)_2Cl_2]\cdot 2H_2O$ in 5 mL of CH_2Cl_2 and 20 mL of C_2H_5-OH, to give 0.152 g of **RuTRu** (77%). ^{1}H NMR: δ 8.80−8.83 (m, 12H), 8.32−8.05 (m, 23H), 7.61−7.56 (m, 11H), 2.67−2.60 (m, 4H), 1.48−1.44 (m, 4H), 1.34−1.27 (m, 4H), 0.91−0.84 (m, 6H). FT-IR (KBr, cm^{-1}): 3006 (s), 2955 (m), 2929 (m), 2861 (w), 2198 (s, C≡C), 1604 (m), 1465 (m), 1446 (m), 1434 (m), 1275 (m), 1261 (m), 836 (vs), 764 (s), 751 (s). UV−vis (CH_3CN; λ, nm (ϵ, M^{-1} cm^{-1})): 286 (119 000), 426 (66 900). ESI-MS (CH_3CN): 1815.3 ($[M - PF_6]^+$, 100%), 835.3 ($[M - 2PF_6]^{2+}$), 508.3 ($[M - 3PF_6]^{3+}$. Anal. Calcd for $C_{76}H_{64}N_{12}Ru_2SP_4F_{24}$: C, 46.59; H, 3.29; N, 8.58. Found: C, 46.27; H, 3.00; N, 8.20.

RuTRuTRu. Prepared according to the general conditions, from 0.070 g (0.074 mmol) of **bpyTbpyTbpy** and 0.124 g (0.236 mmol) of $[Ru(bpy)_2Cl_2]\cdot 2H_2O$ in 20 mL of CH_2Cl_2 and 40 mL of C_2H_5OH, to give 0.186 g of **RuTRuTRu** (82%). ^{1}H NMR: δ 8.90−8.75 (m, 18H), 8.35−8.00 (m, 36H), 7.63−7.59

TABLE 1: Electrochemical Properties of Complexes and References in Solution[a]

	$E_{1/2}$/V (ΔE_p/ mV)	$E_{1/2}$/V (ΔE_p/ mV)				
complex	Ru(II/III)	T−e−bpy−e−T[b]	T−e−bpy[c]	bpy[d]	$\Delta E_{1/2}$/V	E_{MLCT}/eV (estd)
RuT	1.26 (70), 1e$^-$		−1.18 (60), 1e$^-$	−1.50 (60), 1e$^-$ −1.76 (80), 1e$^-$	2.44	1.94
TRuT	1.30 (70), 1e$^-$	−1.02 (60), 1e$^-$		−1.46 (60), 1e$^-$ −1.65 (80), 1e$^-$	2.32	1.83
RuTRu	1.31 (100), 2e$^-$		−1.14 (90), 2e$^-$	−1.44 (80), 2e$^-$ −1.79 (80), 2e$^-$	2.45	1.95
RuTRuTRu	1.31 (100), 3e$^-$	−0.93 (60), 1e$^-$	−1.16 (70), 2e$^-$	−1.39 (80), 3e$^-$ −1.77 (80), 3e$^-$	2.24	1.74
$Ru(bpy)_3^{2+}$	1.27 (70), 1e$^-$			−1.34 (70), 1e$^-$ −1.54 (70), 1e$^-$ −1.79 (75), 1e$^-$	2.61	2.10

[a] Potentials determined by cyclic voltammetry in 0.1 M $TBAPF_6/CH_3CN$ solution, complex concentration $(0.8-1.5) \times 10^{-4}$ M. Potentials were measured at a Pt working electrode referenced to a Pt wire quasi-reference electrode. Potentials were standardized using a ferrocene (Fc) internal reference and are converted to SSCE scale assuming that $E_{1/2}(Fc/Fc^+) = 0.39$ V. [b] Reduction localized on a bipyridine that contains two ethynylthiophene substituents. [c] Reduction localized on a bipyridine that contains one ethynylthiophene substituent. [d] Reduction localized on a 2,2′-bipyridine.

(m, 14H), 2.67−2.59 (m, 8H), 1.48−1.41 (m, 8H), 1.33−1.23 (m, 8H), 0.91−0.84 (m, 12H). FT-IR (KBr, cm^{-1}): 2919 (m), 2851 (m), 2195 (w, C≡C), 1619 (m), 1566 (m), 1463 (m), 1384 (s), 1241 (m), 1121 (w), 840 (vs), 730 (s). UV−vis (CH_3CN; λ, nm (ϵ, M^{-1} cm^{-1})): 286 (189 000), 443 (128 000). ESI-MS (CH_3CN): 1385.3 ($[M - 2PF_6]^{2+}$, 100%), 875.3 ($[M - 3PF_6]^{3+}$), 467.3 ($[M - 5PF_6]^{5+}$). Anal. Calcd for $C_{122}H_{104}N_{18}Ru_3S_2P_6F_{36}$: C, 47.90; H, 3.43; N, 8.24. Found: C, 47.37; H, 3.05; N, 8.02.

Photophysical Measurements. All photophysical studies were conducted in 1 cm square quartz cuvettes on argon bubble-degassed solutions unless otherwise noted. For the emission measurements, sample concentrations were adjusted to produce "optically dilute" solutions (i.e., $A_{max} < 0.20$; typical final concentration is ca. 1.5×10^{-6} M). Transient absorption measurements were performed on solutions with higher concentrations (i.e., $A_{max} \approx 0.8-1.0$ at 355 nm, ca. 7.5×10^{-6} M).

Steady-state absorption spectra were recorded on a Varian Cary 100 dual-beam spectrophotometer or Perkin-Elmer Lambda 900 spectrometer. Corrected steady-state emission measurements were conducted on a SPEX F-112 fluorimeter. Emission quantum yields were measured by relative actinometry, with $Ru(bpy)_3^{2+}$ in argon degassed water ($\phi_{em} = 0.055$) as the actinometer.[42] Time-resolved emission decays were observed with time-correlated single photon counting (FLT, Photochemical Research Associates; excitation source, 405 nm IBH NanoLED-07 diode laser; emission filter, appropriate emission interference filter for the observed emission). Lifetimes were determined from the observed decays with DAS6 fluorescence lifetime deconvolution software (IBH, Glasgow, U.K.). Transient absorption spectra were obtained on previously described instrumentation, with the third harmonic of a Nd:YAG laser (Spectra Physics GCR-14, 355 nm, 10 ns fwhm, 5 mJ $pulse^{-1}$, ≈20 mJ cm^{-2} irradiance) as the excitation source.[43] Primary factor analysis followed by first-order (A → B) least-squares fits of the transient absorption data was accomplished with SPECFIT global analysis software.[44]

Electrochemical Measurements. Electrochemical studies employed cyclic voltammetry with a conventional three-electrode system using a BAS CV-50W voltammetric analyzer equipped with a Pt microdisk (2 mm^2) working electrode and a silver wire counter electrode. Ferrocene was used as an internal standard and was calibrated against a saturated calomel reference electrode (SSCE) separated from the electrolysis cell by a glass frit presoaked with electrolyte solution. Solutions contained the electroactive substrate in deoxygenated and anhydrous acetonitrile containing tetra-*n*-butylammonium hexafluorophosphate as supporting electrolyte. The quoted half-wave potentials were reproducible within 10 mV.

Results and Discussion

Structures. The structures of the complexes that are the focus of the present investigation are illustrated in Chart 1. Monomeric complexes **RuT** and **TRuT** contain a single Ru−bpy chromophore flanked by one or two ethynylene−dibutylthiophene moieties (hereafter we refer to the ethynylene−dibutylthiophene unit as "e−T" and the ethynylene−dibutylthiophene−ethynylene unit as "e−T−e"). Dimeric complex **RuTRu** features two equivalent Ru−bpy units coupled by an e−T−e "spacer". Trimeric complex **RuTRuTRu** contains three Ru−bpy chromophores linked by e−T−e spacers.

The stoichiometry of the complexes is confirmed by integration of the well-defined aliphatic protons (methyl and methylene) relative to the aromatic patterns which appear as multiplets due to the overlapping between the protons of the bridging ligand and the unsubstituted bipyridine moieties. When trisubstituted thiophene subunits are present (i.e., in **RuT** and **TRuT**) a singlet arising from the single thiophene proton is observed at 7.27 ppm which integrates for one and two protons, respectively. The stoichiometry together with the overall charge of the complexes was confirmed by electrospray mass spectroscopy.

An important point is that in the trimer complex the three Ru−bpy units are not equivalent. Specifically, in the terminal Ru−bpy complexes the bridging bipyridine units carry only one e−T substituent, whereas in the central Ru−bpy complex the bridging bipyridine unit is substituted with two e−T groups. To facilitate the interpretation of the electrochemical data presented below, it is also important to recognize that monomer complexes **RuT** and **TRuT** represent, respectively, models for the terminal and central Ru−bpy units in the **RuTRuTRu**. The presence of chemically distinct Ru−bpy units in the trimer is reflected in the electrochemical data presented below.

Electrochemistry and MLCT State Energies. The electrochemical properties of the four complexes were characterized by cyclic voltammetry in CH_3CN solution. Table 1 lists the potentials (relative to the SSCE reference electrode) for the waves that were observed in the +1.9 to −1.6 V window. First, for all of the complexes a single reversible anodic wave was observed in the region between +1.25 and +1.30 V that is due to the Ru(II/III) couple. Note that the Ru(II/III) wave is shifted

slightly positive in **TRuT** compared to **RuT**; this positive shift likely reflects the fact that the e−T subsituents are electron withdrawing, and two e−T substituents have a greater effect than one on the Ru(II/III) potential. In **RuTRu** and **RuTRuTRu** only a single, multielectron wave is resolved for the Ru(II/III) couple, a fact which indicates that the electronic coupling between the metal centers spacers is relatively weak. Importantly, for all of the complexes there is no clear indication of an anodic voltammetric wave within the potential window explored that can be assigned to a thiophene-based oxidation.

All of the complexes exhibit three or more well-resolved reversible waves in the cathodic branch of the voltammograms that are due to reductions centered on the e−T substituted and unsubstituted bipyridine ligands. The entries in the table are organized according to the assignment as to which bipyridine ligand is reduced at the listed potential. For each of the complexes the first reduction is shifted to a more positive potential than the first reduction of $Ru(bpy)_3^{2+}$ (data shown for comparison). This feature clearly indicates that in all of the new complexes the first reduction is localized on the e−T substituted bipyridine ligands. Moreover, there are significant differences in the potentials of the first (and in some cases the second) reduction potentials, which reflects the different electronic environments of bipyridines that contain one or two e−T substituents.

The first reduction of **TRuT** is shifted +160 mV compared to that of **RuT**, while the latter complex features a first reduction potential that is +160 mV relative to that of the parent complex, $Ru(bpy)_3^{2+}$. The cathodic shifts for the first reduction potentials of **RuT** and **TRuT** clearly reflect the combined effects of electron withdrawing and charge delocalization by the e−T substituents. Similar effects were observed in several recent studies of ruthenium complexes that feature 2,2′-bipyridine ligands bearing arylene−ethynylene substituents in the 5,5′-positions.[38,45]

The first reduction of **RuTRu** appears as a single, $2e^-$ wave that is shifted only slightly positive (+40 mV) relative to the corresponding potential in the monomer **RuT**. This similarity reflects the fact that in the dimer the first reduction is localized on the e−T substituted bpy ligands. The fact that the reduction appears as a single wave indicates that the electronic interactions between the two bipyridines which are bridged by the e−T−e unit are not strong.

Trimer **RuTRuTRu** features two separate reductions at potentials that are considerably more positive compared to that of $Ru(bpy)_3^{2+}$. Both of these reductions are localized on the bpy−e−T−e−bpy−e−T−e−bpy oligomeric ligand; however, the fact that it is possible to clearly resolve the first reduction as a $1e^-$ wave and the second as a $2e^-$ wave indicates that the reductions are localized largely on the substituted bpy units (i.e., the electron in the reduced complexes is not delocalized over the entire oligomer ligand). The first wave is assigned to reduction of the "central" bpy ligand which carries two e−T substituents, while the second $2e^-$ wave is assigned to reduction of the "terminal" bpy ligands which each carry a single e−T substituent.

To facilitate interpretation of the photophysical data that is presented below, it is useful to apply the electrochemical data to estimate the energy of the relaxed ^{3}MLCT excited states in the complexes. A considerable body of evidence is available which indicates that the energy of the lowest ^{3}MLCT state in Ru−diimine complexes follows a proportionality of the form, $E_{MLCT} = \Delta E_{1/2} + D$, where E_{MLCT} is the energy of ^{3}MLCT, $\Delta E_{1/2}$ is the difference in the first and oxidation and reduction potentials for the complex, and D is a constant that reflects the sum of the electron−hole interaction energies (e.g., Coulombic, exchange, solvation) in the ^{3}MLCT state.[46] To estimate the relative ordering of the lowest ^{3}MLCT states in the series of thiophene complexes, Table 1 contains a listing of $\Delta E_{1/2}$ values for the complexes, along with estimates for E_{MLCT}, which are derived by assuming $D = 0.5$ eV.[46] Inspection of the estimated E_{MLCT} values reveals that the two complexes which feature bpy ligands bearing only one e−T substituent (**RuT** and **RuTRu**) are expected to have relatively high energy MLCT states, while in the two complexes that contain bpy ligands with two e−T substituents (**TRuT** and **TRuTRuT**) the MLCT state is at a comparatively lower energy. The significance of this ordering of MCLT state energies will become apparent below.

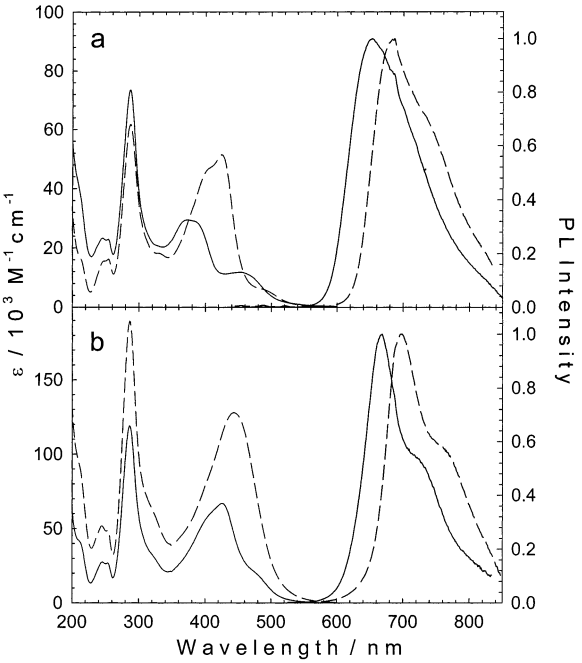

Figure 1. UV−visible absorption (at left, scale at left) and photoluminescence spectra (at right, scale at right) of complexes in CH_3CN solution at ambient temperature. (a) Solid line, **RuT**; dashed line, **TRuT**. (b) Solid line, **RuTRu**; dashed line, **RuTRuTRu**.

UV−Visible Absorption Spectroscopy. Figure 1 illustrates the absorption spectra of the series of Ru complexes in CH_3CN solution and the band maxima and molar absorption coefficients are listed in Table 2. Comparison of the spectra of the individual complexes allows assignment of the various absorption bands to transitions localized on the ancillary 2,2′-bpy ligands, the e−T substituted bpy ligands, and MLCT transitions. All four complexes display a strong, narrow absorption band in the UV at approximately 286 nm. A similar feature is observed in the spectrum of $Ru(bpy)_3^{2+}$, and on this basis the absorption is assigned to the π,π^* transition of the auxiliary 2,2′-bpy ligands. Note that the intensity of this transition increases along the series **RuT** ∼ **TRuT** < **RuTRu** < **RuTRuTRu**, consistent with the fact that the dimer and trimer contain four and six unsubstituted 2,2′-bpy ligands, respectively, while the monomeric complexes contain only two.

In the low-energy region, the spectra of **RuT**, **TRuT**, and **RuTRu** each display strong absorption between 360 and 425 nm and a weaker band (or shoulder) between 450 and 500 nm. The higher energy band is attributed to the long-axis polarized π,π^* transition of the e−T substituted bpy ligand.[14,38,41,45] This assignment is supported by the fact that the band red shifts and its intensity increases with the length of the conjugated ligand.

TABLE 2: Photophysical Properties of Complexes[a]

	absorption		emission								
complex	λ_{max} nm	ϵ_{max} ($mM^{-1}\,cm^{-1}$)	λ_{max}(298K)[b] nm	λ_{max}(80K)[b] nm	E_{oo}(298K)[b] eV	ΔE_s[b] eV	ϕ_{em}	τ_{em}[c] μs	k_r[d] ($10^4\ s^{-1}$)	k_{nr}[d] ($10^6\ s^{-1}$)	τ_{TA}[e] μs
RuT	287	73.5	647	614	1.93	0.10	0.082	1.05	7.8	0.87	1.18
	372	29.5									
	453	11.9									
TRuT	287	61.7	677	653	1.83	0.07	0.035	0.88	4.0	1.10	0.89
	424	51.5									
RuTRu	286	119	670	660	1.85	0.03	0.044	7.32	0.6	0.13	6.71
	426	66.9									
TRuTRuT	286	189	701	686	1.77	0.04	0.021	1.35	1.6	0.73	1.34
	443	128									

[a] Argon outgassed CH_3CN solutions unless otherwise noted. [b] Argon outgassed ethanol/methanol (4/1 (v/v)) solutions. [c] All emission decays were monoexponential, and in each case the quality of the fits was good as evidenced by $\chi^2 < 1.3$. [d] $k_r = \phi_{em}/\tau_{em}$; $k_{nr} = 1/\tau_{em}(1 - \phi_{em})$. It is assumed that emitting excited state is produced with unit efficiency. [e] Transient absorption decay lifetime.

The MLCT absorption appears as a well-resolved band in **RuT** with $\lambda_{max} = 453$ nm; however, in **TRuT** and **RuTRu** the band appears as a shoulder on the more intense π,π^* intraligand transition. Note that the molar absorptivity of the MLCT band is approximately 2-fold greater in **RuTRu**, which is consistent with the presence of two Ru chromophores in the dimer. The MLCT absorption in **RuTRuTRu** is completely obscured by the π,π^* intraligand transition of the bpy−e−T−e−bpy−e−T−e−bpy oligomer ligand. In support of this assignment we note that the visible absorption of **RuTRuTRu** is very similar to that of related Ru complexes that contain thiophene or dioxythiophene units linked to the 5,5′-position of one or more of the bipyridine ligands.[41,45]

Photoluminescence Spectroscopy. Before discussing the photophysical properties of the series of the Ru−thiophene complexes, it is necessary to outline some general features regarding the excited states that are expected to be involved in their photophysics. It is well-established that ruthenium(II)−polypyridyl complexes feature relatively low lying MLCT excited states that are based on Ru → diimine charge transfer.[47,48] MLCT states are typically characterized by a broad photoluminescence band with little or no vibronic structure in the 580−700 nm region.[48,49] Lifetimes for Ru → diimine MLCT states typically range from 0.1 to 1.0 μs,[48] and they usually decrease with emission energy in a manner that is consistent with the energy gap law.[50,51] Radiative and nonradiative decay rates for the MLCT excited state are typically $\approx(0.5-1) \times 10^5$ and $\approx 1 \times 10^6\ s^{-1}$, respectively.[51] Another characteristic of MLCT states is that they display moderate to large outer-sphere reorganization energies (i.e., λ_s typically ranges from 0.05 to 0.1 eV).[52] A measure of λ_s for an MLCT state is obtained from the thermally induced Stokes shift of the emission band, ΔE_s, which is related to the outer-sphere reorganization energy by the expression $\Delta E_s = 2\lambda_s$.[52]

Recently there has been increasing interest in the properties of ruthenium(II)−polypyridyl complexes that contain diimine ligands that are covalently linked to (or an integral part of) a π-conjugated organic chromophore.[53−55] This work has established that when the organic chromophore has a $^3\pi,\pi^*$ state with an energy that is below (or slightly above) that of the Ru → diimine MLCT state, the photoluminescence and transient absorption will arise from the "intraligand" $^3\pi,\pi^*$ state. Several features signal that a $^3\pi,\pi^*$ state is involved in the photophysics of a complex: (1) well-resolved vibronic structure in the photoluminescence, especially at low-temperatures; (2) an emission decay lifetime (τ_{em}) considerably longer than 1 μs; (3) radiative and nonradiative decay rates (k_r and k_{nr}, respectively) that are considerably less than typical for MLCT states; (4) unusually low ΔE_s.

In view of this background, we turn to a discussion of the photoluminescence properties of the ruthenium−thiophene complexes. Figure 1 illustrates the room temperature emission spectra of the four complexes in CH_3CN solution, and Table 2 summarizes a number of important photophysical parameters. The temperature dependence of the photoluminescence spectra was also examined in ethanol/methanol (4:1) solvent (glass). The variable temperature spectra are provided in the Supporting Information, and Table 2 lists the ΔE_s values determined from the variable temperature spectra. Inspection of the photoluminescence data reveals that the complexes fall into two categories: (1) monometallic complexes **RuT** and **TRuT** both feature a broad, nearly structureless emission, with $\tau_{em} \leq 1$ μs; (2) polymetallic complexes **RuTRu** and **RuTRuTRu** both feature a narrower emission band with clearly defined vibronic structure at room temperature, and $\tau > 1$ μs. As outlined in detail below, it is believed that **RuT** and **TRuT** luminesce from the MLCT manifold, while **RuTRu** and **RuTRuTRu** emit from a $^3\pi,\pi^*$ state based on the thiophene−bipyridine oligomer ligands. Because of this difference in properties, the two pairs of complexes are discussed separately below.

The photoluminescence properties of the monometallic complexes **RuT** and **TRuT** are characteristic of an MLCT excited state. First, as noted above, the emission bands are broad and nearly structureless. In addition, the values of τ_{em}, k_r, and k_{nr} for the two complexes are in accord with the MLCT assignment. The emission from **RuT** and **TRuT** is red-shifted relative to that of $Ru(bpy)_3^{2+}$. This red shift is consistent with the fact that the e−T substituted bpy ligands are more easily reduced compared to unsubstituted bpy. Interestingly, the experimentally determined room temperature E_{00} values for **RuT** and **TRuT** (Table 2) are in excellent agreement with the E_{MLCT} values estimated by the electrochemical method (Table 1), where the e−T substituted bpys were assumed to be the acceptor ligands. This correspondence indicates that for **RuT** and **TRuT** the lowest excited state is based on dπ Ru → π^* bpy−e−T (or T−e−bpy−e−T) MLCT. Note that the emission lifetimes (τ_{em}, Table 2) of the two complexes vary as **RuT** > **TRuT**. This trend is in accord with the energy gap law, since the E_{00} values vary as **RuT** > **TRuT**.

In contrast to the monometallic complexes, the photoluminescence properties of polymetallic complexes **RuTRu** and **RuTRuTRu** are atypical for MLCT states. As noted above, the room temperature emission spectra feature a well-resolved vibronic progression which is even better resolved in the 80 K spectra (Supporting Information). Interestingly, the ΔE_s values for **RuTRu** and **RuTRuTRu** are small, indicating that the luminescent excited state is relatively nonpolar, consistent with a $^3\pi,\pi^*$ assignment. The emission decay lifetimes of **RuTRu**

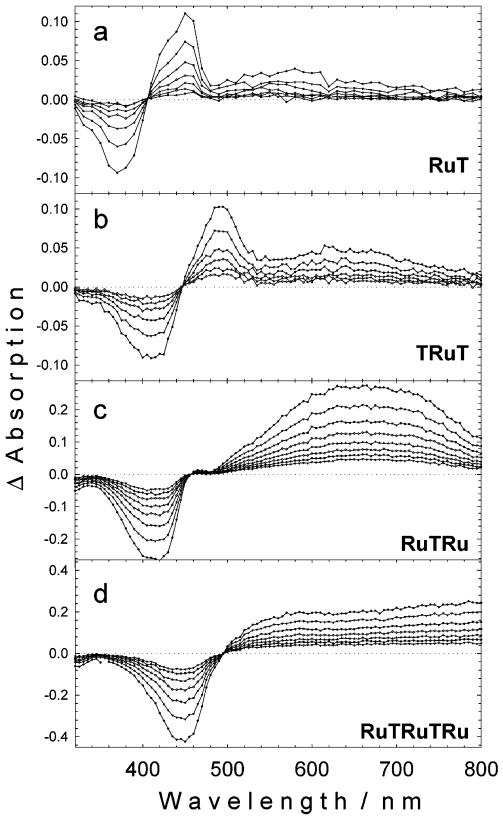

Figure 2. Transient absorption difference spectra for the complexes in argon degassed CH_3CN solution obtained at various delay times following 355 nm pulsed excitation (5 mJ pulse^{-1} dose, 20 mJ cm^{-2} energy density, 10 ns fwhm pulse width). (a) **RuT**, delay times 0−3.2 μs; (b) **TRuT**, delay times 0−1.6 μs; (c) **RuTRu**, delay times 0−16 μs; (d) **RuTRuTRu**, delay times 0−1.6 μs.

and **RuTRuTRu** are also in accord with the $^3\pi,\pi^*$ assignment. Indeed, the dimer has $\tau_{em} = 7.3$ μs, which is an order of magnitude greater than expected if the lowest excited state is MLCT. The enhanced lifetime of **RuTRu** arises because k_r and k_{nr} for the complex are significantly less than in **RuT** and **TRuT**. Interestingly, the lifetime of **RuTRuTRu** is considerably less than that of **RuTRu**. The lower lifetime arises mainly because k_{nr} in **RuTRuTRu** $\approx 5\times$ larger than in **RuTRu**. The difference in nonradiative decay rates is explained by the fact that the $^3\pi,\pi^*$ state is very close in energy to the MLCT state in **RuTRuTRu** (see below).

Transient Absorption Spectroscopy. To further characterize the long-lived excited states produced by photoexcitation of the ruthenium−thiophene complexes, transient absorption (TA) spectroscopy was carried out to elucidate their excited-state spectra. Figure 2 illustrates TA difference absorption spectra of the four complexes produced by a 355 nm excitation pulse, and the lifetimes determined by analysis of the TA decay kinetics (τ_{TA}) are listed in Table 2. Note that for each complex there is good agreement between the lifetimes determined by TA and emission; this correspondence suggests that the transients observed in the TA experiment are the emitting excited states.

The TA spectra for **RuT** and **TRuT** are illustrated in Figure 2a,b, respectively. The TA spectra for the two complexes are qualitatively similar—they are characterized by strong ground-state bleaching and a relatively narrow and intense transient absorption band in the mid-visible region. The TA spectra of **RuT** and **TRuT** are very similar to the TA difference spectra of complexes of the type (L)Ru(bpy)$_2^{2+}$, (L)Re(CO)$_3$Cl, and

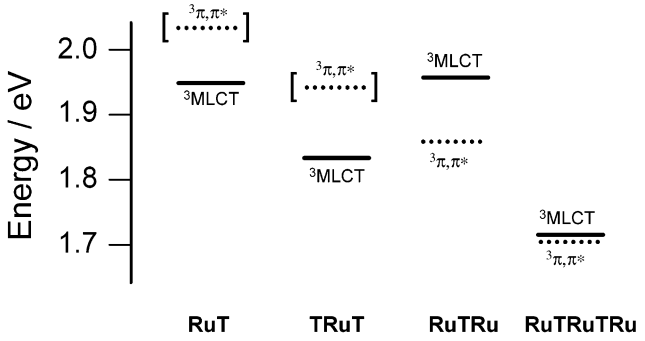

Figure 3. Energies of $^3\pi,\pi^*$ and MLCT excited states for the series of complexes. Estimated as described in text.

(L)Ir(bpy)$_2^+$, where L is a 2,2′-bipyridine ligand that features aryl−ethynyl substituents in the 5,5′-positions.[14,56,57] This similarity is important, because in the other systems the TA spectra have been assigned to dπ M $\rightarrow$ π^* L MLCT excited states.[14,56,57] By analogy, it is believed that the TA spectra of **RuT** and **TRuT** arise from the MLCT states. An interesting point is that the ground-state bleaching bands observed for **RuT** and **TRuT** correspond to the intraligand π,π^* absorption band of the e−T substituted bpy ligands. This confirms the premise that e−T ligands are the acceptor ligands in the MLCT transition. Bleaching of the ground-state MLCT absorption bands is probably not observed because the mid-visible excited-state absorption feature is stronger (i.e., $\Delta\epsilon$ is large) and overwhelms the bleaching of the ground-state MLCT band.

The TA spectra for **RuTRu** and **RuTRuTRu** are illustrated in Figure 2c,d. Interestingly, the spectra for these complexes are distinct compared to the TA spectra of **RuT** and **TRuT**. The spectrum of **RuTRu** features strong ground-state bleaching in the intraligand π,π^* absorption feature, in addition to a broad excited-state absorption band with $\lambda_{max} \approx 650$ nm. The spectrum of **RuTRuTRu** is similar, except that the excited-state absorption appears to extend into the near-IR region. Significantly, the TA spectra of the dimeric and trimeric complexes correspond quite closely to the TA spectra of a series of metal−organic polymers that contain (L)Ru(bpy)$_2^{2+}$ chromophores interspersed within a π-conjugated poly(3-octylthiophene) backbone.[41] In the series of polymers, the excited-state absorption was definitively assigned to the $^3\pi,\pi^*$ state of the poly(thiophene) segments. By analogy, we believe that the TA spectra observed for **RuTRu** and **RuTRuTRu** arise from a $^3\pi,\pi^*$ excited state that is based on **bpyTbpy** and **bpyTbpyTbpy** oligomer ligands. The TA spectrum of **RuTRuTRu** is broader and red-shifted because of the increased conjugation in the oligomer ligand system for this complex. Specifically, the bridging oligomer ligand in **RuTRu** features five heterocyclic rings in conjugation, while the bridging oligomer ligand in **RuTRuTRu** has eight heterocyclic rings.

Excited-State Model. On the basis of the electrochemical, photoluminescence and transient absorption data, the diagram shown in Figure 3 is constructed to illustrate how the energies of the lowest excited states vary along among the series of ruthenium−thiophene complexes. In this diagram the energies of the ^{3}MLCT states are determined by the electrochemical method (Table 1), while those of the $^3\pi,\pi^*$ states are either estimated (shown in brackets in Figure 3) or are based on the emission energies of the complexes that emit from the $^3\pi,\pi^*$ manifold.

Several points are of interest with respect to the energy level diagram. First, as noted above, in complexes that contain a bpy ligand that is flanked by two e−T units (i.e., **TRuT** and **RuTRuTRu**) the ^{3}MLCT state is at a relatively lower energy.

Second, the energy of the $^3\pi,\pi^*$ state is believed to decrease with the conjugation length of the thiophene−bipyridine oligomer ligands. (The conjugation length of the oligomer ligands can be roughly approximated by the number of heterocyclic rings in the π-system.) Specifically, the energy of the $^3\pi,\pi^*$ state is believed to follow the order, **RuT** (3 rings) > **TRuT** (4 rings) > **RuTRu** (5 rings) > **RuTRuTRu** (8 rings), where the number in parentheses indicates the number of heterocyclic rings in the oligomer π-system.

An interesting result of these two effects is that there is a distinct crossover in the lowest excited state for **TRuT** and **RuTRu.** Thus, in **TRuT** the ^{3}MLCT state is stabilized relative to $^3\pi,\pi^*$ because the chromophoric bipyridine ligand is flanked by two e−T units. Thus, this complex features photophysics that are typical of a system having a lowest ^{3}MLCT state. By contrast, in **RuTRu** the ^{3}MLCT state is destabilized relative to the $^3\pi,\pi^*$ state because each of the two chromophoric bipyridine ligands feature only one e−T substituent. In addition, the $^3\pi,\pi^*$ state is at a slightly lower energy than in **TRuT** because of increased conjugation. As a result, in **RuTRu** the energy of the $^3\pi,\pi^*$ state is well below that of ^{3}MLCT, and the observed photophysics are dominated by the intraligand $^3\pi,\pi^*$ state.

As shown in Figure 3, it is believed that in **RuTRuTRu** the $^3\pi,\pi^*$ and ^{3}MLCT states are at almost the same energy. On the basis of the observed photophysics, we conclude that $^3\pi,\pi^*$ is slightly below ^{3}MLCT. However, there is an important result arising from the close energetic proximity of the $^3\pi,\pi^*$ and ^{3}MLCT states. Specifically, nonradiative decay from the $^3\pi,\pi^*$ state is much faster in **RuTRu** than in **RuTRuTRu**. This difference in decay rates arises because the dominant nonradiative decay pathway for the $^3\pi,\pi^*$ states in the two complexes is via (thermally activated) crossing to the ^{3}MLCT state. Nonradiative decay is relatively fast in **RuTRuTRu** because there is little energetic barrier to crossing from $^3\pi,\pi^*$ to ^{3}MLCT. By contrast, in **RuTRu** the ^{3}MLCT state is >0.1 eV above $^3\pi,\pi^*$, and consequently crossing to the ^{3}MLCT manifold is significantly slower.

Photoinduced Electron Transfer with Methyl Viologen. To characterize the electron-transfer properties of the excited-state ruthenium−thiophene complexes, experiments were carried out using *N*,*N*′-dimethyl-4,4′-bipyridinium (MV^{2+}) as an oxidant. In these experiments the efficiency of MV^{2+} quenching of the excited-state complexes was determined by using transient absorption spectroscopy. In addition, transient absorption difference spectra were obtained to characterize the absorption properties of the electron-transfer products. A key objective of these studies was to determine whether the quenching efficiency is strongly influenced by the nature of the lowest excited state (i.e., ^{3}MLCT vs $^3\pi,\pi^*$).

Rate constants for bimolecular quenching of the excited-state complexes (k_q) were determined by measuring the decay rate of the excited-state complexes as a function of MV^{2+} concentration (i.e., Stern−Volmer plots). The quenching rate constants, k_q, are collected in Table 3, along with estimates for the excited-state oxidation potentials of the complexes, $E_{1/2}(*Ru^{2+}/Ru^{3+})$, and the driving force for excited-state electron transfer to MV^{2+}, $\Delta G_{ET} = E_{1/2}(*Ru^{2+}/Ru^{3+}) - E_{1/2}(MV^{2+}/MV^{\bullet+})$. In each case MV^{2+} was observed to quench the excited states, and as demonstrated by transient absorption spectroscopy (see below), the quenching arises due to electron transfer from the excited-state complex to MV^{2+} as exemplified for **RuT**,

$$*[(bpy)_2Ru(bpy{-}e{-}T)]^{2+} + MV^{2+} \rightarrow [(bpy)_2Ru(bpy{-}e{-}T)]^{3+} + MV^{\bullet+} \quad (1)$$

TABLE 3: Photoinduced Electron-Transfer Data[a]

complex	$E_{1/2}(*Ru^{2+}/Ru^{3+})$[b]/V	ΔG_{ET}[c]/eV	k_q[d]/(10^7 M^{-1} s^{-1})
RuT	−0.67	−0.22	39
TRuT	−0.53	−0.08	17
RuTRu	−0.54	−0.13	5.1
RuTRuTRu	−0.46	−0.01	3.6

[a] All data for CH_3CN solutions. [b] Oxidation potential for excited-state complex, potential vs SCE. [c] Free energy for photoinduced electron transfer to MV^{2+}, $E_{1/2}(MV^{2+}/MV^{\bullet+}) = -0.45$ V. [d] Excited-state quenching rate constants determined by Stern−Volmer quenching experiments carried out by transient absorption spectroscopy.

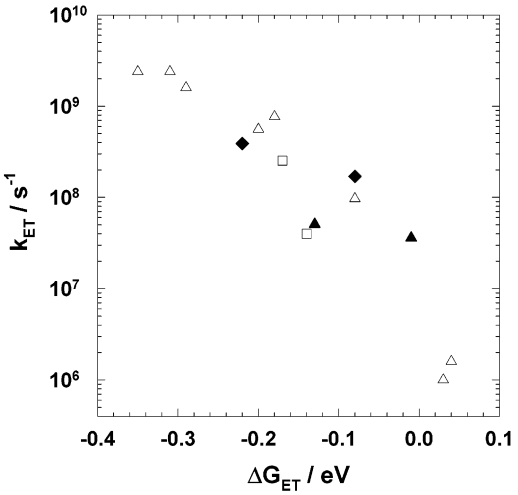

Figure 4. Plot of log k_{ET} vs ΔG_{ET} for electron-transfer quenching (Marcus Plot): (△) $Ru(bpy)_3^{2+}$ quenched by a series of organic electron acceptors (data from ref 58); (□) ruthenium−thiophene complexes from ref 41 quenched by MV^{2+}; (◆) **RuT** and **TRuT** quenched by MV^{2+}; (▲) **RuTRu** and **RuTRuTRu** quenched by MV^{2+}.

The quenching rate constants listed in Table 3 are not corrected for Coulombic effects that might be expected to influence the rates due to the difference in charge on the complexes (i.e., **RuT** and **TRuT** are dications, **RuTRu** is a tetracation, and **RuTRuTRu** is a hexacation).[58,59] However, it was found that the k_q's for all of the complexes were virtually unchanged when the quenching studies were carried out in the presence of tetrabutylammonium hexafluorophosphate (0.1 M), and on the basis of this finding is it concluded that the difference in charge on the complexes has a minimal effect on the differences in quenching rates.

Comparison of the data in Table 3 shows that the k_q values generally increase with electron-transfer driving force. Figure 4 illustrates a plot of k_q vs ΔG_{ET} for the series of ruthenium−thiophene complexes, plotted along with quenching data taken from the literature for $Ru(bpy)_3^{2+}$ and for another series of thiophene-substituted Ru complexes.[41,58] Although there is some scatter, the data for the new series of complexes qualitatively fit the correlation defined by the other series of Ru complexes. On the basis of this comparison, we conclude that the nature of the lowest excited state (i.e., $^3\pi,\pi^*$ or MLCT) for the ruthenium−thiophene complexes does not have a strong influence on the rate of electron-transfer quenching.

Figure 5 illustrates transient absorption spectra obtained at delay times ranging from 0 to 1.6 μs after excitation for solutions of the ruthenium−thiophene complexes with added MV^{2+}. In each case, the spectra at early times are the same as those shown in Figure 2, which have been assigned to the excited-state complexes. However, at later delay times, the spectra evolve in shape and a "long-time" spectrum is observed which persists long after excitation (>10 μs). The species which give rise to

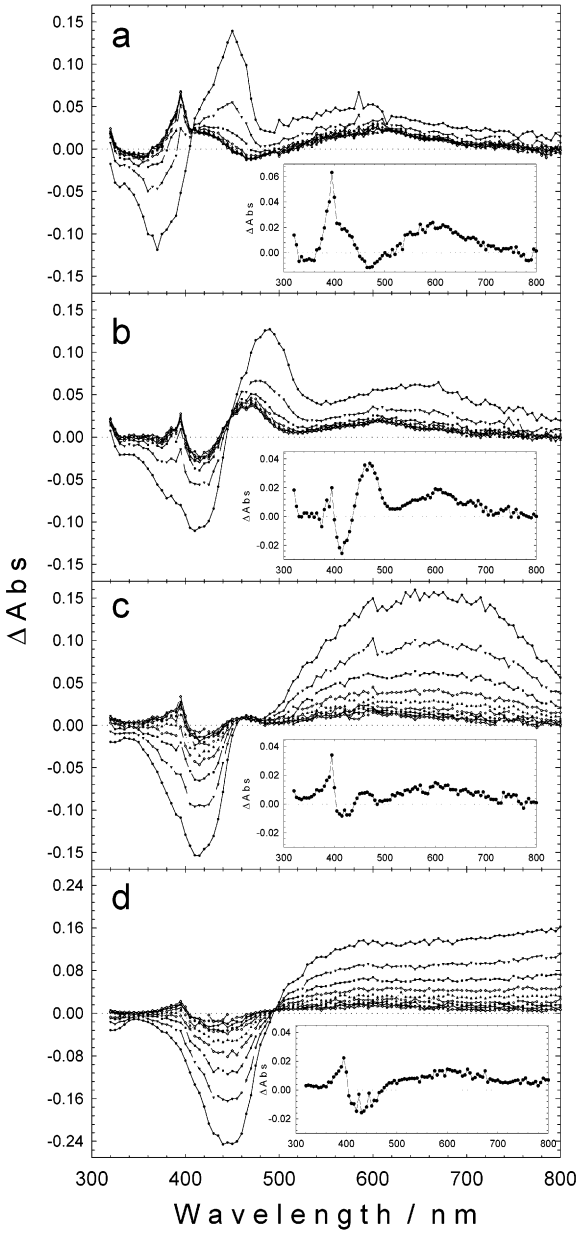

Figure 5. Transient absorption difference spectra for complexes with in argon degassed CH_3CN with solution MV^{2+}. In the main panels spectra are obtained at delay times ranging from 0 to 1.6 μs following the excitation pulse. The expansions shown in the insets were obtained at 1.6 μs delay. (a) **RuT** with MV^{2+} (c = 16 mM). (b) **TRuT** with MV^{2+} (c = 30 mM). (c) **RuTRu** with MV^{2+} (29 mM). (d) **RuTRuTRu** with MV^{2+} (c = 48 mM).

the long-time spectrum decay according to equal concentration, second-order kinetics on a time scale of 20−50 μs. The long-time spectrum is believed to arise from a superposition of the absorption spectra of the products of photoinduced electron transfer, i.e., the oxidized ruthenium−thiophene complex and $MV^{\bullet+}$. The insets in Figure 5 illustrate the long-time spectra more clearly, and some interesting features emerge when these spectra are compared. Specifically, these spectra provide information regarding the electronic structure of the one-electron oxidized ruthenium−thiophene complexes.

For **RuT**, the long-time spectrum is dominated by absorption at λ_{max} = 395 and 605 nm along with a weak ground-state bleach at λ_{min} = 480 nm. Clearly the absorption features that dominate the long-time difference spectrum for the **RuT**/MV^{2+} system arise from $MV^{\bullet+}$, which is known to absorb at 395 nm ($\epsilon \approx$ 30 000 M^{-1} cm^{-1}) and 605 nm ($\epsilon \approx$ 10 000 M^{-1} cm^{-1}).[60] This fact indicates that any bands arising from oxidized **RuT** are comparatively weak ($\Delta\epsilon$ < 5000 M^{-1} cm^{-1}). On the basis of this observation, it is believed that the "hole" in the oxidized complex resides on the metal center and not on the bpy−e−T ligand; i.e., the structure of oxidized **RuT** is $[(bpy)_2Ru^{III}(bpy-e-T)]^{3+}$. This conclusion is supported by the fact that the long-time spectrum features modest bleaching in the region of the ground-state MLCT absorption band. In addition, if the bpy−e−T ligand were oxidized, a relatively strong visible absorption band would be expected on the basis of the fact that thiophene-containing oligomers typically feature strong visible absorption bands in the oxidized state.[41,61,62] The structure $[(bpy)_2Ru^{III}(bpy-e-T)]^{3+}$ is consistent with the electrochemistry (Table 1), which showed that the first oxidation of **RuT** arises from the Ru(II/III) couple. An additional point of note is the fact that there is only modest change in the absorption of **RuT** when the Ru center is oxidized from the II to the III oxidation state. This indicates that the oxidation of the metal center has only a modest effect on the energy and intensity of the long-axis π,π^* absorption band which is localized on the bpy−e−T ligand.

CHART 2

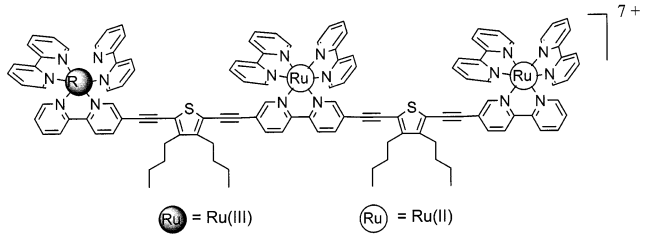

The long-time spectrum observed for the **TRuT**/MV^{2+} system (Figure 5b, inset) is distinct from that of **RuT**/MV^{2+}. In particular, although the features for $MV^{\bullet+}$ are present at 390 and 605 nm, the spectrum is dominated by a derivative shaped bleach-absorption feature with λ_{min} = 415 nm and λ_{max} = 465 nm. On the basis of the relative intensity of the 465 nm absorption relative to the 395 nm $MV^{\bullet+}$ absorption ($\Delta\epsilon \approx$ 30 000 M^{-1} cm^{-1}), it is clear that the 465 nm band is very strong with $\Delta\epsilon \approx$ 50 000 M^{-1} cm^{-1}. On the basis of the fact that the electrochemistry indicates that the first oxidation of **TRuT** is due to the Ru(II/III) couple, it is believed that the structure of the oxidized complex is $[(bpy)_2Ru^{III}(T-e-bpy-e-T)]^{3+}$. Further, we posit that the derivative-shaped band arises from a red shift in the long-axis π,π^* absorption band which is localized on the T−e−bpy−e−T ligand. Apparently the band red shifts due to the electronic effect of Ru(III) center, which is considerably more electron deficient compared to Ru(II). Similar effects have been observed concomitant with one-electron oxidation of transition metal complexes of bipyridine-containing π-conjugated systems.[41,63,64]

The long-time difference spectra of the **RuTRu**/MV^{2+} and **RuTRuTRu**/MV^{2+} systems are very similar to that of **RuT** (Figure 5c,d, insets). The correspondence for **RuTRu** is not surprising, since with respect to the metal complex the chromophoric units are the same in these two complexes. However, the similarity between the long-time spectra in the case of the trimer is significant, because it signals that in the one electron oxidized complex the hole resides on one of the terminal Ru units (Chart 2). This result is not surprising, because analysis of the electrochemical data suggests that the e−T substituents are electron withdrawing (see above) and serve to slightly increase the potential for the Ru(II/III) couple. Therefore, it is expected that in **RuTRuTRu** the Ru(II/III) couple for the central

Ru ion will be at a slightly higher potential compared to that for the terminal Ru ions.

Summary and Conclusions

The electrochemical and photophysical properties of a new series of ruthenium−polypyridine complexes that contain ethynyl-linked, 3,4-dibutylthiophene-substituted bipyridine ligands have been thoroughly investigated. The e−T-substituted bipyridine ligands are reduced at considerably lower oxidation potentials compared to the unsubstituted bipyridine ligands. As a result, the e−T substituted ligands act as "acceptors" for the low-energy dπ (Ru) → π^* (L) MLCT excited states. Absorption spectra of the complexes feature relatively low energy transitions arising from long-axis polarized π,π^* transitions localized on the e−T-substituted bipyridine ligands. The intensity of the π,π^* transitions increases with the length of the "oligomer" ligands, and in the case of **TRuT** and **RuTRuTRu**, the transitions dominate the low-energy region of the absorption spectra. The photophysical properties of the complexes are dominated by relatively long-lived, photoluminescent excited states. Analysis of the photophysical data indicates that for **RuT** and **TRuT** the lowest excited state is based on a ^{3}MLCT configuration where the e−T-substituted ligand acts as the acceptor, while for **RuTRu** and **RuTRuTRu** the lowest excited state is $^3\pi,\pi^*$ based on the oligomer ligands. All of the complexes undergo efficient photoinduced electron transfer with MV^{2+}, and the dynamics of the electron-transfer quenching are not strongly affected by the nature of the long-lived excited state. Transient absorption spectroscopy provides spectroscopic data for the one-electron oxidized complexes, and analysis of the spectral features provides information concerning the electronic structure of the oxidized complexes.

This study provides considerable insight concerning the interaction between MLCT and "ligand-localized" $^3\pi,\pi^*$ excited states in metal complexes that contain π-conjugated ligands. In particular, the results make it clear that when the lowest excited state is energetically well-separated from the next higher energy configuration, the characteristics of the excited state are dominated by the lowest configuration. Thus, when the lowest state is MLCT and the $^3\pi,\pi^*$ state is considerably higher in energy, the observed photophysics are very "typical" for a MLCT configuration (i.e., microsecond lifetime, broad structureless emission, etc.). By analogy, when the lowest state is $^3\pi,\pi^*$ and the MLCT state is considerably higher in energy, the photophysics are dominated by the $^3\pi,\pi^*$ configuration (i.e., considerably enhanced lifetime, structured emission, low radiative rate, broad, intense transient absorption, etc.). On the other hand, when the intraligand and charge-transfer manifolds are close in energy, the photophysics appear to be a composite of the two states. While it is possible that the two states retain their identity and the observed properties arise due to an excited-state equilibrium, it is more likely that the states undergo configuration mixing. More information on this effect will be gained in future studies where we use ligand design to carefully "tune" the energy of the MLCT state relative to that of the $^3\pi,\pi^*$ state. Results of such studies will be reported in a forthcoming manuscript.

Acknowledgment. Work carried out at the University of Florida was supported by funding from the U.S. National Science Foundation (Grant No. CHE-0211252), and the work performed at ECPM/ULP was supported by the Centre National de la Recherche Scientifique (CNRS), the French Ministery of Research, and the IST/ILO EC Contract 2001-33057.

Supporting Information Available: Variable temperature photoluminescence spectra of the ruthenium−thiophene complexes. This material is available free of charge via the Internet at http://pubs.acs.org.

References and Notes

(1) This manuscript is dedicated to Prof. Michael Kasha. His contributions to our understanding of the triplet state play an important role in the work described herein.

(2) Skotheim, T. A., Elsenbaumer, R. L., Reynolds, J. R., Eds. *Handbook of Conducting Polymers*, 2nd ed.; Dekker: New York, 1998.

(3) McGehee, M. D.; Miller, E. K.; Moses, D.; Heeger, A. J. In *Advances in Synthetic Metals. Twenty Years of Progress in Science and Technology*; Bernier, P., Lefrant, S., Bidan, G., Eds.; Elsevier: Amsterdam, 1999; pp 98−205.

(4) Burroughes, J. H.; Bradley, D. D. C.; Brown, A. R.; Marks, R. W.; Mackay, K.; Friend, R. H.; Burn, P. L.; Holmes, A. B. *Nature* **1990**, *347*, 539−541.

(5) Yu, G.; Gao, J.; Hummelen, J. C.; Wudl, F.; Heeger, A. J. *Science* **1995**, *270*, 1789−1791.

(6) Groenendaal, B. L.; Jonas, F.; Freitag, D.; Pielartzik, H.; Reynolds, J. R. *Adv. Mater.* **2000**, *12*, 481−494.

(7) Chen, L.; McBranch, D. W.; Wang, H.-L.; Helgeson, R.; Wudl, F.; Whitten, D. G. *Proc. Natl. Acad. Sci. U.S.A.* **1999**, *96*, 12287−12292.

(8) Gaylord, B. S.; Heeger, A. J.; Bazan, G. C. *Proc. Natl. Acad. Sci. U.S.A.* **2002**, *99*, 10954−10957.

(9) Wang, Q.; Yu, L. *J. Am. Chem. Soc.* **2000**, *122*, 11806−11811.

(10) Wang, Q.; Wang, L.; Yu, L. *J. Am. Chem. Soc.* **1998**, *130*, 12860−12868.

(11) Peng, Z.; Yu, L. *J. Am. Chem. Soc.* **1996**, *118*, 3777−3778.

(12) Ng, P. K.; Gong, X.; Chan, S. H.; Lam, L. S. M.; Chan, W. K. *Chem.-Eur. J.* **2001**, *7*, 4358−4367.

(13) Wilson, J. S.; Dhoot, A. S.; Seeley, A. J. A. B.; Khan, M. S.; Kohler, A.; Friend, R. H. *Nature* **2001**, *413*, 828−831.

(14) Walters, K. A.; Ley, K. D.; Cavalaheiro, C. S. P.; Miller, S. E.; Gosztola, D.; Wasielewski, M. R.; Bussandri, A. P.; van Willigen, H.; Schanze, K. S. *J. Am. Chem. Soc.* **2001**, *123*, 8329−8342.

(15) Walters, K. A.; Dattelbaum, D. M.; Ley, K. D.; Schoonover, J. R.; Meyer, T. J.; Schanze, K. S. *Chem. Commun.* **2001**, 1834−1835.

(16) Liu, Y.; Li, Y.; Schanze, K. S. *J. Photochem. Photobiol. C: Photochem. Rev.* **2001**, *3*, 1−23.

(17) Encinas, S.; Flamigni, L.; Barigelletti, F.; Constable, E. C.; Housecroft, C. E.; Schofield, E. R.; Figgemeier, E.; Fenske, D.; Neuburger, M.; Vos, J. G.; Zehnder, M. *Chem.-Eur. J.* **2002**, *8*, 137−150.

(18) Pappenfus, T. M.; Mann, K. R. *Inorg. Chem.* **2001**, *40*, 6301−6307.

(19) Lamansky, S.; Djurovich, P.; Murphy, D.; Abdel-Razzaq, F.; Lee, H. E.; Adachi, C.; Burrows, P. E.; Forrest, S. R.; Thompson, M. E. *J. Am. Chem. Soc.* **2001**, *123*, 4304−4312.

(20) Kwong, R. C.; Sibley, S.; Dubovoy, T.; Baldo, M.; Forrest, S. R.; Thompson, M. E. *Chem. Mater.* **1999**, *11*, 3709−3713.

(21) Welter, S.; Brunner, K.; Hofstraat, J. W.; De Cola, L. *Nature* **2003**, *421*, 54−57.

(22) Staromlynska, J.; McKay, T. J.; Bolger, J. A.; Davy, J. R. *J. Opt. Soc. Am. B* **1998**, *15*, 1731−1736.

(23) McKay, T. J.; Staromlynska, J.; Davy, J. R.; Bolger, J. A. *J. Opt. Soc. Am. B* **2001**, *18*, 358−362.

(24) Peng, Z.; Gharavi, A. R.; Yu, L. *J. Am. Chem. Soc.* **1997**, *119*, 4622−4632.

(25) McCullough, R. D.; Lowe, R. D. *J. Chem. Soc., Chem. Commun.* **1992**, 70−72.

(26) Bauerle, P.; Fischer, T.; Bidlingmeier, B.; Stabel, A.; Rabe, J. P. *Angew. Chem., Int. Ed. Engl.* **1995**, *34*, 303−307.

(27) Lovinger, A. J.; Rothberg, L. J. *J. Mater. Res.* **1996**, *11*, 1581−1592.

(28) Loewe, R. S.; Khersonsky, S. M.; McCullough, R. D. *Adv. Mater.* **1999**, *11*, 250−253.

(29) Kodaira, T.; Watanabe, A.; Ito, O.; Watanabe, M.; Saito, H.; Koishi, M. *J. Phys. Chem.* **1996**, *100*, 15309−15313.

(30) Becker, R. S.; de Melo, J. S.; Maçanita, A.; Elisei, F. *J. Phys. Chem.* **1996**, *100*, 18683−18695.

(31) de Melo, J. S.; Silva, L. M.; Arnaut, L. G.; Becker, R. S. *J. Chem. Phys.* **1999**, *111*, 5427−5433.

(32) Bennati, M.; Grupp, A.; Mehring, M.; Bauerle, P. *J. Phys. Chem.* **1996**, *100*, 2849−2853.

(33) Xu, B.; Holdcroft, S. *Adv. Mater.* **1994**, *6*, 325−327.

(34) Rothe, C.; Hintschich, S.; Monkman, A. P.; Svensson, M.; Anderson, M. R. *J. Chem. Phys.* **2002**, *116*, 10503−10507.

(35) Harriman, A.; Khatyr, A.; Ziessel, R.; Benniston, A. C. *Angew. Chem., Int. Ed.* **2000**, *39*, 4287−4290.

(36) Harriman, A.; Mayeux, A.; De Nicola, A.; Ziessel, R. *Phys. Chem. Chem. Phys.* **2002**, *4*, 2229−2235.
(37) Ley, K. D.; Whittle, C. E.; Bartberger, M. D.; Schanze, K. S. *J. Am. Chem. Soc.* **1997**, *119*, 3423−3424.
(38) Wang, Y.; Liu, S.; Pinto, M. R.; Dattelbaum, D. M.; Schoonover, J. R.; Schanze, K. S. *J. Phys. Chem. A* **2001**, *105*, 11118−11127.
(39) Liu, Y.; Jiang, S.; Glusac, K.; Powell, D. H.; Anderson, D. F.; Schanze, K. S. *J. Am. Chem. Soc.* **2002**, *124*, 12412−12413.
(40) De Nicola, A.; Liu, Y.; Schanze, K. S.; Ziessel, R. *Chem. Commun.* **2003**, 288−289.
(41) Walters, K. A.; Trouillet, L.; Guillerez, S.; Schanze, K. S. *Inorg. Chem.* **2000**, *39*, 5496−5509.
(42) Harriman, A. *J. Chem. Soc., Chem. Commun.* **1977**, 777−778.
(43) Wang, Y. S.; Schanze, K. S. *Chem. Phys.* **1993**, *176*, 305−319.
(44) Stultz, L. K.; Binstead, R. A.; Reynolds, M. S.; Meyer, T. J. *J. Am. Chem. Soc.* **1995**, *117*, 2520−2532.
(45) Zhu, S. S.; Kingsborough, R. P.; Swager, T. M. *J. Mater. Chem.* **1999**, *9*, 2123−2131.
(46) Vlcek, A. A.; Dodsworth, E. S.; Pietro, W. J.; Lever, A. B. P. *Inorg. Chem.* **1995**, *34*, 1906−1913.
(47) Demas, J. N.; Crosby, G. A. *J. Mol. Spectrosc.* **1968**, *26*, 72−77.
(48) Juris, A.; Balzani, V.; Barigelletti, F.; Campagna, S.; Belser, P.; von Zelewsky, A. *Coord. Chem. Rev.* **1988**, *84*, 85−277.
(49) Lees, A. J. *Chem. Rev.* **1987**, *87*, 711−743.
(50) Caspar, J. V.; Meyer, T. J. *J. Phys. Chem.* **1983**, *87*, 952−957.
(51) Barqawi, K. R.; Murtaza, Z.; Meyer, T. J. *J. Phys. Chem.* **1991**, *95*, 47−50.
(52) Chen, P. Y.; Meyer, T. J. *Chem. Rev.* **1998**, *98*, 1439−1477.
(53) Simon, J. A.; Curry, S. L.; Schmehl, R. H.; Schatz, T. R.; Piotrowiak, P.; Jin, X.; Thummel, R. P. *J. Am. Chem. Soc.* **1997**, *119*, 11012−11022.
(54) Tyson, D. S.; Castellano, F. N. *J. Phys. Chem. A* **1999**, *103*, 10955−10960.
(55) Tyson, D. S.; Bialecki, J.; Castellano, F. N. *Chem. Commun.* **2000**, 2355−2356.
(56) Li, Y.; Whittle, C. E.; Walters, K. A.; Ley, K. D.; Schanze, K. S. In *Electronic, Optical and Optoelectronic Polymers and Oligomers*; Jabbour, G. E., Meijer, E. W., Sariciftci, N. S., Swager, T. M., Eds.; Materials Research Society: Warrendale, PA, 2002; Vol. 665, pp 61−72.
(57) Glusac, K. D.; Jiang, S.; Schanze, K. S. *Chem. Commun.* **2002**, 2504−2505.
(58) Bock, C. R.; Connor, J. A.; Gutierrez, A. R.; Meyer, T. J.; Whitten, D. G.; Sullivan, B. P.; Nagle, J. K. *J. Am. Chem. Soc.* **1979**, *101*, 4815−4824.
(59) Sutin, N. *Prog. Inorg. Chem.* **1983**, *30*, 441−498.
(60) Kosower, E. M.; Cotter, J. C. *J. Am. Chem. Soc.* **1964**, *86*, 5524−5527.
(61) Caspar, J. V.; Ramamurthy, V.; Corbin, D. R. *J. Am. Chem. Soc.* **1991**, *113*, 600−610.
(62) Wintgens, V.; Valat, P.; Garnier, F. *J. Phys. Chem.* **1994**, *98*, 228−232.
(63) Manas, E. S.; Chen, L. X. *Chem. Phys. Lett.* **2000**, *331*, 299−307.
(64) Li, Y. Ph.D. Dissertation, University of Florida, Gainesville, FL, 2001.